



Applications of anisotropic slipline theory with non-uniform lattice rotation

Animesh Pandey and Anurag Gupta

Abstract. Anisotropic slipline theory, with non-uniform lattice rotation field, is used to discuss new slipline solutions for the plane strain problems of punch indentation and mode 1 stationary crack in a ductile single crystal with piecewise linear yield locus. The proposed solution allows for both linear dislocation arrays and sectors with bulk dislocation density. Such features provide considerable latitude in the number of allowable stress discontinuities, and their orientation, when compared to the solutions which assume uniform lattice rotation.

Mathematics Subject Classification. 74C05 · 74R20.

Keywords. Anisotropic slipline theory, Lattice rotation, Plastic spin, Punch indentation, Mode 1 crack, Dislocation density.

1. Introduction

The formalism of plane strain, elastically rigid, incompressible, perfect plasticity, otherwise known as slipline theory, has a unique mathematical structure such that the governing partial differential equations remain hyperbolic for all stress values during plastic deformation [5,6]. This allows us to gain considerable analytical insight into the solutions of a variety of physical problems posed using the slipline theory [9,13,18]. The assumption of elastic rigidity restricts elastic deformation to be a lattice rotation field. The rotation field can be eliminated as long as it remains constant throughout the solid [7]. It is for this reason that lattice rotation is ignored both in the well-studied isotropic slipline theory [5,6,9] and in the anisotropic slipline theory at incipient plastic flow [15]. The lattice rotation field is otherwise non-uniform in anisotropic solids and cannot be neglected [7]. Moreover, incorporating it in the plasticity theory is tantamount to prescribing plastic spin as a constitutive function [3,7]. We also note that the non-uniformity in lattice rotation field gives rise to a non-trivial geometrically necessary dislocation distribution in the solid. In particular, a discontinuity in the lattice rotation field creates a dislocation wall, which is equivalently a grain boundary in the present situation, whereas its gradient represents a continuous distribution of dislocations [7].

The purpose of this brief note is to construct new solutions of some classical problems in anisotropic slipline theory by incorporating a non-uniform lattice rotation field, which was hitherto ignored in previously developed anisotropic slipline models [8,15] and their applications [11]. The present work can be used to explain certain experimental observations for stress field distribution around a crack tip in single crystals [1,2,10] and for deformation fields in plane strain indentation test on single crystals [12]. In the former, angular sectors of uniform stress, separated by lines of stress discontinuity, are observed around the crack tip. Existing theories (such as [16]) fall short in the correct prediction of the number of sectors, the inclination of discontinuity lines, the existence of boundaries with a jump in lattice rotation field, and the dependence of solution on crack tip orientation. By incorporating non-uniform lattice rotation field in the slipline theory, some of these experimental predictions can be justified in the proposed framework.

In Sect. 2, we summarize the governing equations of anisotropic slipline theory while emphasizing the nature of discontinuities in stress, velocity, and rotation fields. We discuss in detail the nature of solution

in a region where the stress state belongs to a vertex of the yield locus. Subsequently, in Sect. 3, we use the anisotropic slipline theory to revisit the classical problems of plane punch indentation and mode I stationary crack in a ductile single crystal.

2. Anisotropic slipline theory

Under plane strain assumption, the velocity field is taken of the form $\mathbf{v} = u\mathbf{e}_1 + v\mathbf{e}_2$ with components u and v dependent only on the in-plane components $x = \mathbf{x} \cdot \mathbf{e}_1$ and $y = \mathbf{x} \cdot \mathbf{e}_2$ of the position vector \mathbf{x} . Here, unit vectors $\{\mathbf{e}_1, \mathbf{e}_2, \mathbf{e}_3\}$ form a fixed right-handed orthonormal basis. The lattice rotation field is assumed to have axis along \mathbf{e}_3 and is hence completely determined by a scalar field $\gamma = \gamma(x, y, t)$, where t denotes time. γ represents the angular change in the lattice orientation measured anticlockwise with respect to the \mathbf{e}_1 -axis. As noted before, spatial gradient of γ quantifies bulk dislocation density field, away from any curves of γ discontinuity in the plane, whereas the jump in γ across any such curve represents a surface dislocation density field [7]. Let $\boldsymbol{\sigma} = \sigma_{ij}\mathbf{e}_i \otimes \mathbf{e}_j$ denote the symmetric Cauchy stress tensor such that the components σ_{ij} are all independent of the out-of-plane spatial variable. Let σ_1 and σ_2 be the in-plane principal stresses and \mathbf{u}_1 and \mathbf{u}_2 be the corresponding principal directions of the Cauchy stress. Let θ be the angle between \mathbf{e}_1 and \mathbf{u}_1 measured anticlockwise from the former. Hence, $\sigma_{11} - \sigma_{22} = (\sigma_1 - \sigma_2) \cos 2\theta$ and $2\sigma_{12} = (\sigma_1 - \sigma_2) \sin 2\theta$. Due to the non-trivial lattice rotation field, the second Piola–Kirchhoff stress, say \mathbf{S} , is distinct from the Cauchy stress. In fact, in terms of the components $S_{ij} = \mathbf{S} \cdot \text{Sym}(\mathbf{e}_i \otimes \mathbf{e}_j)$, $S_{11} - S_{22} = (\sigma_1 - \sigma_2) \cos(2\theta - 2\gamma)$, and $2S_{12} = (\sigma_1 - \sigma_2) \sin(2\theta - 2\gamma)$.

We will first collect the governing equations away from curves with discontinuous fields. The equilibrium equations, neglecting body forces and inertia, are given by

$$\partial_x \sigma_{11} + \partial_y \sigma_{12} = 0 \text{ and } \partial_x \sigma_{12} + \partial_y \sigma_{22} = 0, \quad (1)$$

where ∂_x is the partial derivative with respect to x , etc. The yield criterion is assumed to be of the form $F(\mathbf{S}) = 0$, where F is continuously differentiable. Under plane strain assumption, it reduces to [7]

$$\sigma_1 - \sigma_2 = 2k(\theta - \gamma), \quad (2)$$

where k , a continuously differentiable function of its argument, denotes the maximum shear stress. The deviation from circularity in the polar plot $(k(\theta - \gamma), 2(\theta - \gamma))$, such as those shown in Figs. 1 and 4a, represents anisotropy in the yield behavior. For isotropic solids, k is constant while for anisotropic solids, with uniform lattice rotation, it is only a function of θ . It should be noted that although the yield locus is fixed in the space of second Piola–Kirchhoff stress, it can vary in the Cauchy stress space parameterized by

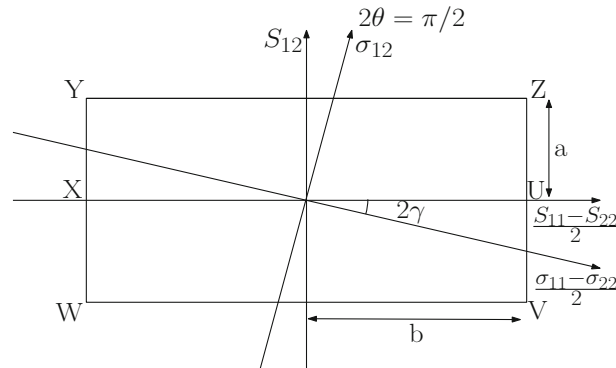


FIG. 1. Rectangular yield locus

γ . Such dependence characterizes a *geometric* hardening (or softening) which appears due to the rotation of crystal slip systems with respect to the material axes. The plastic incompressibility condition, due to the absence of elastic strains, is given by

$$\partial_x u + \partial_y v = 0. \quad (3)$$

The symmetric part of the plane strain plastic flow rule, upon using (2), reduces to [7]

$$2\partial_x u \cos(2\theta + 2\psi) + (\partial_y u + \partial_x v) \sin(2\theta + 2\psi) = 0, \quad (4)$$

where ψ is defined from $k' = 2k \cot 2\psi$. The superscript prime denotes the partial derivative of k with respect to $(\theta - \gamma)$. Accordingly, 2ψ is the anticlockwise inclination of the tangent to the polar plot with respect to the radial direction. The skew part of the flow rule is given by [7]

$$2 \frac{\Omega_{21} \sin(2\psi)}{\sin(2\theta + 2\psi)} \partial_x u + \partial_y u - \partial_x v + 2\partial_t \gamma + 2u\partial_x \gamma + 2v\partial_y \gamma = 0, \quad (5)$$

where Ω_{21} is a constitutively prescribed plastic spin field and ∂_t is the partial derivative with respect to t . We refer the interested reader to Gupta and Steigmann [7] for a detailed derivation of the above relations. The six governing Eqs. (1)–(5) are used to solve for three in-plane stress components, two velocity components, and lattice rotation angle. Note that Eq. (5) appears due to considerations of lattice rotation and plastic spin. The existing anisotropic slipline theories ignore both of these factors; in particular, they assume k to be a function of only θ .

We allow for discontinuities in stress, velocity, and lattice rotation fields (and their gradients) within plastic regions or at the boundary of rigid and plastic regions. The jumps in stress and velocity fields across a discontinuity curve in the plane, with normal $\mathbf{n} = \sin \phi \mathbf{e}_1 - \cos \phi \mathbf{e}_2$, satisfy equations of equilibrium

$$[[\sigma_{11}]] \sin \phi - [[\sigma_{12}]] \cos \phi = 0 \text{ and } [[\sigma_{12}]] \sin \phi - [[\sigma_{22}]] \cos \phi = 0, \quad (6)$$

and incompressibility

$$[[u]] \sin \phi - [[v]] \cos \phi = 0, \quad (7)$$

where $[[\cdot]] = (\cdot)^+ - (\cdot)^-$ denotes the jump across the curve, with superscripts \pm as the limiting value of the field as it approaches the curve from the regions into which \mathbf{n} and $-\mathbf{n}$ are directed, respectively. The two relations in (6), combined with (2), give an equation for the slope of the discontinuity curve

$$\cot(2\phi - 2\langle\theta\rangle) = \frac{[[k]] \cot[[\theta]]}{2\langle k \rangle}, \quad (8)$$

where $\langle \cdot \rangle = ((\cdot)^+ + (\cdot)^-)/2$ is the average across the curve. The velocity and stress jumps cannot coincide across a curve when the yield locus is strictly convex. Indeed, consider $F(\langle \mathbf{S} \rangle) = 0$ as the yield locus for points on the discontinuity curve. The dissipation at the curve is given by $\langle \boldsymbol{\sigma} \rangle \cdot ([[\mathbf{v}]]) \otimes \mathbf{n}$ [7]. Hence, if $F(\langle \mathbf{S} \rangle) < 0$, the interface remains rigid implying $\text{sym}([[\mathbf{v}]]) \otimes \mathbf{n} = 0$ or equivalently, using (7), $[[\mathbf{v}]]) = 0$. On the other hand, it is clear that velocity and stress jumps can coincide across curves where the limiting bulk stresses in the neighboring points belong to a vertex or an edge of the yield locus. Consequently, such coincidence is prohibited in the isotropic theory but permissible in the anisotropic slipline theory.

For the purpose of the present article, we will assume γ to be known at a given time instant. The stress and velocity solution for a given γ can then be substituted into (5) to determine the evolution of γ . The stress equations (1)–(2) and the velocity Eqs. (3)–(4), both strictly hyperbolic, are decoupled from each other. Moreover, for a stress state away from the vertex on the yield locus, both have coinciding characteristic directions given by $\theta + \psi_\alpha$ (α -lines) and $\theta + \psi_\beta$ (β -lines), where $\psi_{\alpha,\beta}$ are roots of $k' = 2k \cot 2\psi$ such that $\psi_\beta = \psi_\alpha + \pi/2$ and $\psi_{\alpha,\beta} \in [-\pi/2, \pi/2]$. In particular, $2\psi_\beta$ is the anticlockwise angle from the radial direction to the tangential direction of the polar plot $(k(\theta - \gamma), 2\theta - 2\gamma)$. The α and β -lines are collectively called sliplines. The normal forms associated with stress and velocity equations are given in Gupta and Steigmann [7].

We will restrict our attention to polygonal yield contours, such as those shown in Figs. 1 and 4a. Each edge of these piecewise linear contours has a distinct $k(\theta - \gamma) = C |\sin(2\eta_0 - 2(\theta - \gamma))|^{-1}$, where C is a material constant and $2\eta_0$ is the constant anticlockwise inclination of the outward normal to the edge with respect to the positive S_{12} -axis [7]. When the stress states in a plastic region lie on the same linear segment (edge) of the yield locus, the sliplines are two families of curves inclined at η (α -lines) and $\eta + \pi/2$ (β -lines) with respect to \mathbf{e}_1 . The angle 2η is the anticlockwise inclination of the outward normal to the edge with respect to the positive σ_{12} -axis on the polar plot. Interestingly, $\eta = \gamma + \eta_0$, and hence, the curvature of the sliplines is identical to that of the *glide lines*. The glide lines are a family of two mutually orthogonal curves, each with a spatial distribution of edge-type dislocations of same sign [14], along which the dislocations undergo pure gliding. For stress states belonging to an edge, stress discontinuity curves coincide necessarily with either a slipline or a γ discontinuity (this is not true when we consider strictly convex yield contours [7]). Note that, since $[\![\gamma]\!] = [\![\eta]\!]$, lattice rotation cannot be discontinuous across a slipline in such regions.

For a plastic region whose stress state belongs to a vertex on the yield contour, the second Piola–Kirchhoff stress is fixed, but $\sigma_{11} - \sigma_{22}$ and σ_{12} remain variable due to non-uniformity of γ . The vertex state can be thought of as the intersecting state of two linear yield loci characterized by a constant value of $(\theta - \gamma)$. Clearly, γ discontinuities in such a region necessarily coincide with (Cauchy) stress discontinuities. The stress equations are again strictly hyperbolic with characteristic curves inclined at $\theta \pm \pi/4$. The curvature of these characteristic curves, given in terms of the gradient of θ , is related to the gradient of γ and hence to a distribution of dislocation density in the region. The characteristic curves associated with velocity equations (sliplines) are, however, no longer identical to those of stress [7]. The γ discontinuity curves in the considered region can also coincide with the sliplines. The slope of such curves, say ϕ , is related to $[\![\gamma]\!]$ according to the criteria $\phi - \eta_2 \leq [\![\gamma]\!] \leq \phi - \eta_1$, where $2\eta_1$ and $2\eta_2$ (such that $\eta_1 \leq \eta_2$) are angles extended by the outward normal, measured anticlockwise with respect to $2\theta = \pi/2$ line on the polar plot, to the two linear segments which intersect at the vertex. Indeed, each vertex defines an admissible range for the slipline angles by the inclination of the outward normals to the two constraints that intersect at the vertex. Due to the change $[\![\gamma]\!]$ in the lattice rotation, the outward normals reorient themselves at $2\eta_1 + 2[\![\gamma]\!]$ and $2\eta_2 + 2[\![\gamma]\!]$, respectively. The admissible range for slope of α -lines is therefore from $\eta_1 + [\![\gamma]\!]$ to $\eta_2 + [\![\gamma]\!]$.

We would like to note that, in general, γ discontinuities do not coincide with streamlines. They coincide only in very restricted situations with strong assumptions on the continuity of velocity and plastic spin fields in addition to assuming that such interfaces remain stationary. This is contrary to what was proposed in Gupta and Steigmann [7].

3. Examples

3.1. Punch indentation

A flat-ended, rigid, frictionless punch is considered to be indenting on half plane of a ductile single crystal; see Fig. 2a. On the surface below the indenter, $\sigma_{12} = 0$ and $\theta = 0$, and on the free surface, $\sigma_{12} = 0$, $\sigma_{22} = 0$, and $\theta = \pm\pi/2$. The y -velocity component of material points on AB is equal to the downward punch velocity. The isotropic slipline solution to this problem, as provided by Prandtl, is symmetric about the central line of the indenter, consisting of triangular regions of uniform stress below the indenter surface and the free surface [9]. There is a centered fan zone with continuous non-uniform stress field connecting the two uniform stress regions. The indentation pressure associated with yielding for this solution is $k_1(2 + \pi)$, where k_1 is the radius of the circular yield locus. Our aim is to construct anisotropic slipline solutions for the indentation problem with a rectangular yield locus, as shown in Fig. 1. Two distinct stress solutions for the anisotropic problem can be obtained depending on whether the lattice rotation

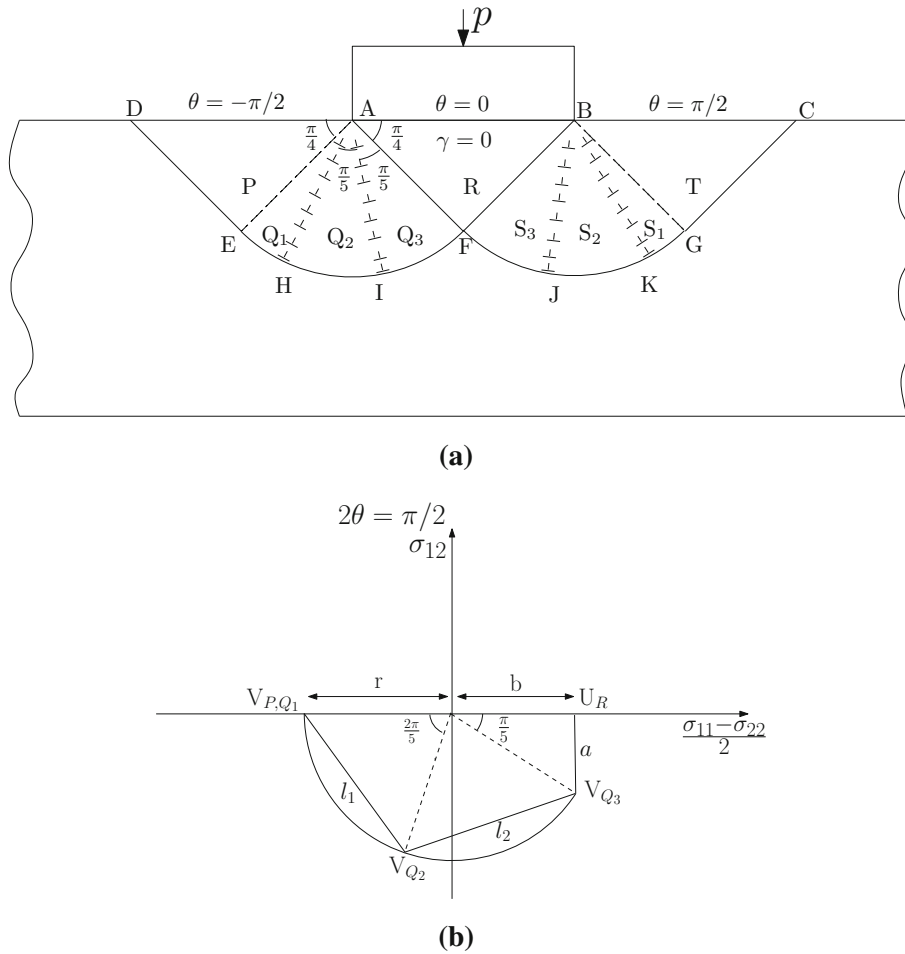


FIG. 2. **a** Slipline solution with minimum number of γ jumps for $\tan^{-1} \frac{a}{b} = \frac{\pi}{5}$, assuming $\gamma = 0$ at AB . **b** Cauchy stress states in different sectors of the punch indentation solution connected with linear chords. The notation U_R , etc., indicates that the stress state in region R corresponds to point U on the yield locus

field γ is prescribed below the indenter (Fig. 2a) or left arbitrary at all the boundaries (Fig. 3); these are discussed below. The velocity solution for the anisotropic problem remains similar to the isotropic case. It is symmetric about the center line of the indenter, with regions P, T , and R (see Figs. 2a, 3) of uniform velocity directed along ED , along GC , and downward, respectively. Regions Q , given by $Q_1 \cup Q_2 \cup Q_3$ in Fig. 2a and by $Q_1 \cup Q_2 \cup Q_3 \cup Q_4$ in Fig. 3, and S , given by $S_1 \cup S_2 \cup S_3$ in Fig. 2a and by $S_1 \cup S_2 \cup S_3 \cup S_4$ in Fig. 3, have a velocity with vanishing component in the radial direction. The velocity field is discontinuous along lines AF and BF .

For a stress discontinuity curve, such that the stress state lies on the same vertex across the jump, (8) implies that $\phi = \langle \theta \rangle \pm \pi/4$. Recall that, at such stress discontinuities, $[[\gamma]] = [[\theta]]$. Considering the case with $\phi = \langle \theta \rangle + \pi/4$ (the other case is similar), the rectangular yield locus in Fig. 1 and the flow rules on each side of the stress jump require that $\pi/4 \leq \phi$ and $\pi/4 + [[\gamma]] \leq \phi$. Hence, $[[\theta]] \leq \langle \theta \rangle$. The relation $2\langle \theta \rangle = \tan^{-1} \frac{a}{b} + [[\theta]]$, which follows from the geometry of the yield locus assuming $a \leq b$, can be then used to conclude that $[[\theta]] \leq \tan^{-1} \frac{a}{b}$ or equivalently $[[\gamma]] \leq \tan^{-1} \frac{a}{b}$. In other words, for any solution

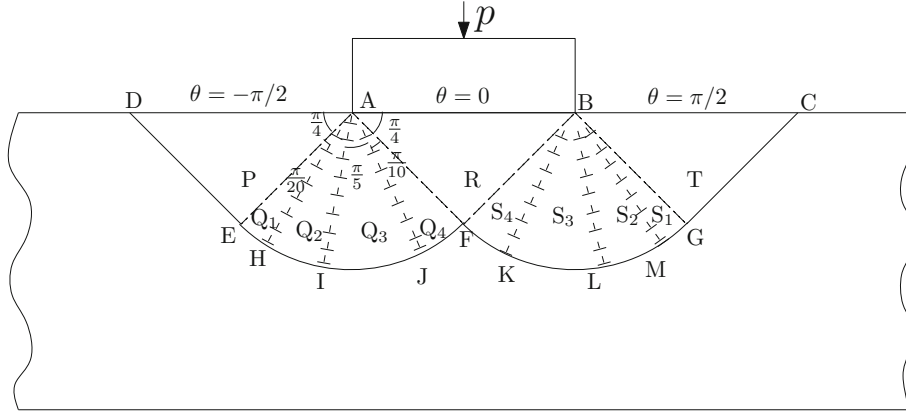


FIG. 3. Slipline solution with minimum number of γ jumps for $\tan^{-1} \frac{a}{b} = \frac{\pi}{5}$, without prescribing γ anywhere on the boundary

with stress state on a single θ vertex of the rectangular yield locus, the maximum allowable value of $[\![\gamma]\!]$ is $\tan^{-1} \frac{a}{b}$.

First, we construct a stress solution by fixing the lattice orientation at the surface below the indenter, such that $\gamma = 0$ on AB (see Fig. 2a). The piecewise uniform solution for stress and γ fields is symmetric about the central line of the indenter with three triangular regions P, R, and T, of uniform stress and γ , such that $\theta_P - \theta_R = -\pi/2$. The symmetry in the slipline solutions is due to the symmetry of the loading and the yield locus. The triangular regions are connected through the intermediate regions Q and S; see Fig. 2a. Across lines AF and BF, stress is discontinuous, but γ is continuous, such that the stress state in regions R, Q, and S corresponds to points U, V, and Z, respectively, on the yield locus. The stress state in regions P and T belongs to the vertex V and Z, respectively. As a result, $(\theta - \gamma)$ remains constant in $P \cup Q$ and $T \cup S$. Regions Q and S contain a finite number of radial lines of γ and (Cauchy) stress discontinuity. These lines, shown as AI, AH, BJ, and BK in Fig. 2a, are accordingly represented as dislocation walls. They divide the intermediate regions Q and S each into three angular sectors with uniform stress and lattice rotation. In our solution, the number of sectors dividing Q and S is decided so as to minimize the number of γ discontinuity lines in the intermediate zone. Indeed, the boundary condition on θ requires that the sum of all γ jumps is necessarily $(\pi - \tan^{-1} \frac{a}{b})/2$. Hence, the lowest number of γ discontinuity lines in each intermediate sector is

$$n = \left\lceil \left(\frac{\pi - \tan^{-1} \frac{a}{b}}{2 \tan^{-1} \frac{a}{b}} \right) \right\rceil, \quad (9)$$

where $\lceil \cdot \rceil$ denotes the least integer function. Any solution with n or more γ discontinuity lines in the intermediate zone is admissible.

A different solution is obtained if we do not impose any boundary conditions on γ . Such a consideration allows us to construct solutions where the entire plastic region has a stress state belonging to one vertex of the yield locus. The solution shown in Fig. 3, for instance, has a stress state corresponding to vertex V on the yield locus given in Fig. 1. Accordingly, $(\theta - \gamma)$ is constant over the entire plastically deforming region. In particular, sectors P, R, and T have uniform stress and γ fields. Both Q and S contain γ discontinuity lines across which (Cauchy) stress is also discontinuous. These are shown as dislocation walls in Fig. 3. The number of sectors in Q and S is again decided in order to minimize the number of γ discontinuity

curves. The lowest number of γ discontinuity lines in each intermediate sector is now given by

$$n = \left\lceil \frac{\pi}{2 \tan^{-1} \frac{a}{b}} \right\rceil. \quad (10)$$

Note that the slipline solution in Fig. 3 does not have any discontinuity lines across which stress is discontinuous but γ continuous. Moreover, contrary to the previous case, we can also construct asymmetric slipline solutions in the present scenario in addition to the symmetric solution shown in Fig. 3. This is due to the freedom in choosing a γ value below the indenter. Interestingly, for the same reason, one can also construct a symmetric slipline solution for an asymmetric yield locus.

We digress briefly to calculate the indentation pressure associated with the solutions outlined above. We show that indentation pressure $p = -(\sigma_{22})_R$, where the subscript R indicates the region, where the stress component is to be evaluated, is the sum of the length of chords associated with each γ jump, in addition to $(a + b + r)$, where $r = \sqrt{a^2 + b^2}$. First, we note that, for the two stress states across a discontinuity line, traction continuity (6) implies $[\![\sigma]\!]^2 - l^2 = 0$, where $\sigma = (\sigma_{11} + \sigma_{22})/2$ is the mean stress and $l^2 = [(\sigma_{11} - \sigma_{22})/2]^2 + [\![\sigma_{12}]\!]^2$ is length-square of the straight chord connecting the two stress states in the Cauchy stress space on the polar plot. Hence, either $[\![\sigma]\!] - l = 0$ or $[\![\sigma]\!] + l = 0$. Our solution in Fig. 2a, in conjunction with traction continuity conditions, admits the latter. Referring to Fig. 2b, which shows stress state in various sectors and the connecting chords, and using $(\sigma)_P = -r$, we can obtain $p = r + b + a + l_1 + l_2$. This expression can be simplified to the form $p = (a + b + r + 4r \sin \frac{\pi}{5})$. We can similarly calculate the indentation pressure for the solution in Fig. 3 as $p = (2r + 4r \sin \frac{\pi}{5} + 2r \sin \frac{\pi}{10})$. Clearly, the solution with minimum number of γ jumps also minimizes the indentation pressure.

Each radial dislocation wall within the intermediate sectors Q and S, in the solutions above, can be replaced by an angular sector with a continuous distribution of dislocation density. This is an alternative way to account for the non-uniformity in lattice rotation and Cauchy stress. In such sectors, γ and stress field both vary continuously over the angular coordinate while remaining constant in the radial direction. The stress state in the intermediate sectors would still belong to one vertex of the yield locus. In general, one can have both dislocation walls and sectors with dislocation distribution; their arrangement would always be such that the θ boundary condition is satisfied.

Finally, we recall the slipline solution from Rice [15] for the same problem as considered above, which assumed a uniform lattice rotation field. This solution consists of sectors with uniform stress states belonging to different vertices of the yield contour punctuated by lines of stress discontinuity (see also [17]). Due to a uniform γ field, there is no possibility of incorporating bulk and surface dislocation density fields in the solution. Moreover, the edges in the yield locus uniquely determine the possible angles at which stress discontinuities can occur thereby fixing the number of sectors of uniform stress in the solution. This constraint is relaxed in our solutions as described above. The indentation pressure is $(4b + 2a)$, which is always less than that of our solutions with non-uniform lattice rotation field. The slipline solutions are symmetric due to the symmetry of the loading and the yield locus. For an asymmetrical yield locus, as shown by Rice [15], the slipline solutions will also be asymmetrical.

3.2. Stationary crack

We consider a mode I stationary crack in a ductile single-crystal solid such that, on crack flanks AC, $\sigma_{12} = 0$, $\sigma_{22} = 0$, and $\theta = \pi/2$, whereas, on the crack propagation line AB, $\sigma_{12} = 0$ and $\theta = 0$. We are interested in the asymptotic behavior of the stress close to the crack tip where the stress field is predominantly a function of the angular position. The solution to this problem, as suggested by Rice [16] for an hexagonal yield locus (see Fig. 4a) and uniform lattice orientation field, is analogous to the punch indentation solution with a similar yield locus, i.e., angular sectors of uniform stress separated by radial lines originating from the crack tip. In this solution, there are four sectors with three stress discontinuity lines on one side of the crack. Moreover, the angle of radial discontinuity lines is fixed by

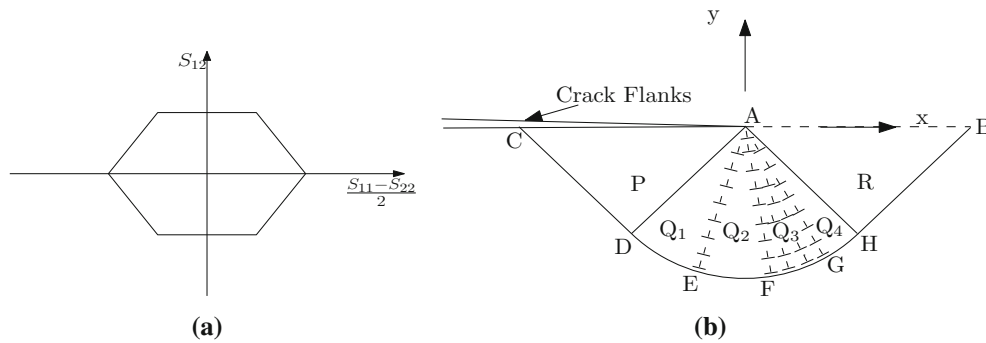


FIG. 4. **a** Hexagonal yield locus. **b** Crack solution for non-uniform lattice orientation. The solution is symmetric with respect to x axis

the slipline direction corresponding to the linear segment across which the jump occurs. Due to uniform lattice orientation, this solution has a trivial dislocation density field associated with it. Experimental observations [1, 2, 10] agree with the general structure of the solution suggested by Rice [16] with sectors of uniform stress separated by radial discontinuity lines. However, there is a disagreement on the radial angle of discontinuity lines, the number of sectors, the existence of γ discontinuity lines, and on the dependence of the solution on crack tip orientation. In fact, the theory proposed by Rice [16] necessarily requires stress discontinuity lines (where stress jumps from one vertex to the other keeping lattice orientation constant) at fixed angles unless certain angular sectors around the crack tip are assumed to remain elastic [4]. Moreover, the experiments also make note of stress discontinuities involving jump in lattice orientation.

As with the punch indentation problem, allowing for non-uniform lattice orientation relaxes several restrictions imposed by the solution proposed by Rice [16]. We show one solution of the anisotropic problem with non-uniform γ in Fig. 4b. The centered fan region has angular regions with piecewise uniform distribution of stress and γ fields. The stress state in the whole sector meanwhile remains on a single vertex of the yield locus. The stress discontinuity lines at fixed radial angles in [16] can be replaced by γ discontinuity lines (for instance, AE in Fig. 4b). The γ discontinuity lines have greater flexibility with respect to their radial angles. Additionally, the solution can also contain angular regions of non-uniform stress and γ , where γ is radially uniform, but changes with the angular coordinate (sector Q₃ in Fig. 4b). Within our framework, in general, there is considerable latitude in the number of stress discontinuities and their orientation. Furthermore, a stress discontinuity can now arise between stress states jumping from one vertex to another (as considered by Rice [16]) and also at γ discontinuity lines with stress state remaining on a single vertex (such as those observed experimentally [10]).

References

1. Crone, W.C., Shield, T.W.: Experimental study of the deformation near a notch tip in copper and copper–beryllium single crystals. *J. Mech. Phys. Solids* **49**, 2819–2838 (2001)
2. Crone, W.C., Shield, T.W., Creuziger, A., Henneman, B.: Orientation dependence of the plastic slip near notches in ductile fcc single crystals. *J. Mech. Phys. Solids* **52**, 85–112 (2004)
3. Dafalias, Y.F.: Plastic spin: necessity or redundancy?. *Int. J. Plast.* **14**, 909–931 (1998)
4. Drugan, W.J.: Asymptotic solutions for tensile crack tip fields without kink-type shear bands in elastic-ideally plastic single crystals. *J. Mech. Phys. Solids* **49**, 2155–2176 (2001)
5. Geiringer, H.: Some recent results in the theory of an ideal plastic body. *Adv. Appl. Mech.* **3**, 197–294 (1953)
6. Geiringer, H.: Ideal plasticity. In: Truesdell, C. *Encyclopedia of Physics*, VIa/3, pp. 403–533. Springer, Berlin (1973)
7. Gupta, A., Steigmann, D.J.: Plane strain problem in elastically rigid finite plasticity. *Q. J. Mech. Appl. Math.* **67**, 287–310 (2014)
8. Hill, R.: The theory of plane plastic strain for anisotropic metals. *Proc. R. Soc. A* **198**, 428–437 (1949)

9. Hill, R.: *The Mathematical Theory of Plasticity*. Oxford University Press, New York (1950)
10. Kysar, J.W., Briant, C.L.: Crack tip deformation fields in ductile single crystals. *Acta Mater.* **50**, 2367–2380 (2002)
11. Kysar, J.W., Gan, Y.X., Mendez-Arzuza, G.: Cylindrical void in a rigid-ideally plastic single crystal. part I: Anisotropic slip line theory solution for face-centered cubic crystals. *Int. J. Plast.* **21**, 1481–1520 (2005)
12. Murthy, T.G., Huang, C., Chandrasekar, S.: Characterization of deformation field in plane-strain indentation of metals. *J. Phys. D Appl. Phys.* **41**, 074026 (2008)
13. Nye, J.F.: The flow of glaciers and ice-sheets as a problem in plasticity. *Proc. R. Soc. A* **207**, 554–572 (1951)
14. Nye, J.F.: Some geometrical relations in dislocated crystals. *Acta Metall.* **1**, 153–162 (1953)
15. Rice, J.R.: Plane strain slip line theory for anisotropic rigid/plastic materials. *J. Mech. Phys. Solids* **21**, 63–74 (1973)
16. Rice, J.R.: Tensile crack tip fields in elastic-ideally plastic crystals. *Mech. Mater.* **6**, 317–335 (1987)
17. Shoemaker, E.M.: A theory of linear plasticity for plane strain. *Arch. Ration. Mech. Anal.* **14**, 283–300 (1963)
18. Tapponnier, P., Molnar, P.: Slip-line field theory and large-scale continental tectonics. *Nature* **264**, 319–324 (1976)

Animesh Pandey and Anurag Gupta
Department of Mechanical Engineering
Indian Institute of Technology, Kanpur 208016
India
e-mail: ag@iitk.ac.in

(Received: April 13, 2016; revised: May 18, 2016)